Int. J. Nanosci. Nanotechnol., Vol. 18, No. 3, Sept. 2022, pp. 157-166

Employing Synthesized MgO-SiO_2 Nanoparticles as Catalysts in Ethanol Conversion to 1,3-Butadiene

Hayder A. Alalwan[1,*], Alaa H. Alminshid[2], Malik M. Mohammed[3], Saif Ali Mohammed Hussein[4] and Mohammed Fakhir Mohammed[5,6,7,8]

[1]Department of Petrochemical Techniques, Technical Institute-Kut, Middle Technical University, Baghdad, Iraq
[2]Department of Chemistry, Wasit University, Kut, Wasit, Iraq
[3]Chemical Engineering and Petroleum Industries Department, Al-Mustaqbal University College, Babel, Iraq
[4]Department of Medical Laboratory Technique, Dijlah University College, Iraq
[5]Kut University Collage, Al Kut, Wasit, Iraq
[6]Al-Turath University College
[7]Islamic University Centre for Scientific Research, The Islamic University, Najaf, Iraq
[8]Osol Aldeen University College, Baghdad, Iraq

(*) Corresponding author: hayder.alalwan@mtu.edu.iq
(Received: 27 November 2021 and Accepted: 12 April 2022)

Abstract

MgO-SiO_2 nanoparticle catalyst was prepared, characterized, and evaluated in a fixed-bed reactor for ethanol conversion to 1,3 butadiene (BD) process (ETB). The prepared catalyst was characterized by XRD, XPS, SEM, TEM, EDS, and BET techniques. The data obtained from the surface and bulk characterizations of the prepared catalyst was used to correlate the catalyst morphology and surface chemistry to its performance in ETB. This work investigates the effect of temperature, Hourly space velocity, and water content on ethanol conversion and product selectivity. In addition, MgO-SiO_2 pellets with size of 500 µm was prepared and applied into the process to evaluate the impact of the catalyst's particle size on its efficiency. The catalyst stability was investigated at the optimum reaction conditions for ten hours of the reaction. 1,3-butadiene selectivity of as high as 60% is achieved at the optimum reaction temperature of 400 ^oC. This high selectivity was attributed to the catalyst's high surface area and surface functional groups. Increasing the reaction temperature increases the rate of ethylene formation and, therefore, the selectivity for acetaldehyde decreases. Increasing the feed flow rate inhibits the formation of BD and increases the acetaldehyde selectivity. The presence of water was found to be a reducer agent to the BD selectivity due to its emphasis on acetone formation. This work investigated the impact of reducing the MgO-SiO_2 catalyst particle size to the nanoscale and provides insightful information about the correlation MgO-SiO_2 catalyst properties with its performance in converting ethanol to BD.

Keywords: *Multifunctional catalysis, Aldol condensation, ETB, Heterogeneous catalysis.*

1. INRODUCTION

Ethanol is considered a valuable raw material for the chemical industry due to its broad conversion ability into commodity chemicals such as 1,3- butadiene, avoiding using petroleum derivatives [1, 2]. The process of ethanol conversion to 1,3-butadiene (BD) or ETB process has attracted much attention due to its wide involvement in various industrial production processes such as synthetic rubbers, polymer resins, and elastomers as well as biofuel production [3]. This process is getting increasing attention as an alternative process to BD extraction from naphtha cracking [4], which considers a sensitive process that can cause a BD shortage [5]. In addition, ETP is an economically competitive process. It has

several advantages in terms of ecology, especially when utilizing ethanol–aqueous mixtures synthesized by inexpensive biomass processing, which considers more profitable and environmentally friendly than using C6 sugars as a source raw material [6-8]. Specifically, the formation of one mole of BD involves consuming four moles of CO_2 in biomass photosynthesis. Therefore, this process will help to consume CO_2 and minimize its high environmental level [9, 10].

Several kinds of catalysts were investigated such as ZnO-Al_2O_3, Ta_2O_5/SiO_2, Mn/sepiolites, Zr(1.5 %), Zn(0.5 %)/SiO_2 , $Cu_{(1\%)}$-$Zr_{(1\%)}$-$Zn_{(1\%)}/SiO_2$, and later a better selective catalyst based on MgO-SiO_2 was developed [11-14]. The development of a more active catalyst correlates to its composition and the technology of its production [15, 16]. Specifically, the catalyst must contain dehydrogenation (oxidation-reduction) functional groups as well as acid-base active sites in a ratio that is specified by the respective properties of the composition of the catalyst components [17]. The partial dehydrogenation of ethanol leads to the form of acetaldehyde (AA)-ethanol mixture**,** followed by converting this mixture into BD [17]. The literature shows that this type of catalyst is best for this reaction due to the suitable integration of strong basal sites, necessary for ethanol activation, with medium-strength acid sites required for the dehydration alkenols to butadiene [1].

Using MgO/SiO_2 catalyst in the ETB process results in a BD yield of 9–42%, with selectivity between 30 to 84% [3]. Washing or impregnating the $MgO–SiO_2$ catalyst with NaOH to minimize the acidic sites showed better BD yields [12]. Several dopants such as zinc, manganese, chromium, nickel, copper, and silver have been investigated to enhance $MgO–SiO_2$ catalyst performance and selectivity. Their contribution in small amounts enhances the activity and selectivity of the catalysts for BD synthesis [3]. Some of these dopants were found to have only limited enhancement on the catalyst performance, while others showed considerable improvement in the yield of BD [18, 19].

Although there is much work in this field, there is still a lack of investigation the impact of dropping the catalyst size to the nanoscale on BD yield and selectivity. Such a dropping would increase the surface area available to the reaction and increase the activity of the catalyst [20]. Thus, in this work, $MgO–SiO_2$ nanoparticles have been synthesized and characterized to evaluate their performance in the ETB process. The results of this investigation provide insight into information about the surface chemistry of catalyst nanoparticles and their correlation to the catalyst's performance in the ETB process.

2. MATERIALS AND METHODS

2.1. Materials and Catalyst Preparation

MgO/SiO_2 nanoparticles were prepared by mixing 0.6 g of resorcinol (>99.5%, Sinoreagent Company) with 0.84 ± 0.01 ml of formaldehyde (>37% Sigma Aldrich) and 12 ± 0.2 ml of aqueous ammonia (>28%, Sinoreagent Company). The mixture was then added to a solution of 140 ml ethanol (>99.9 %, Sigma Aldrich) and 20 ml deionized water. The mixture was stirred continuously for five hours at ambient temperature, followed by adding 2.5 ml of tetraethoxysilane (TEOS; >28.4% SiO_2, Sinoreagent Company) to the solution. Then, the solution was stirred for five minutes, followed by adding 2.5 ml of formaldehyde and 1.5 g of resorcinol and $Mg(NO_3)_2.6H_2O$ (>99%, Sigma Aldrich) where the weight ratio of $Mg(NO_3)_2$ to TEOS was 50%. The mixture was stirred for another two hours, and the product was finally filtered, and washed with ethanol and an unused spray bottle was used to spray the solution on a glass plate with dimensions of 250 × 250 × 3 mm^3. Then it was left to dry in air at 45 ^oC overnight and calcined at 500 ^oC for four hours. To evaluate the impact of the

catalyst's particle size on its efficiency, the resulted powder was pressed under 15 bars into tablets in the size of 500 µm.

2.2. Characterization of Prepared Catalyst

The bulk of the prepared catalyst was scanned by powder X-ray diffraction (XRD) using a Bruker D8 DaVinci system diffractometer. Kratos Axis Ultra X-ray photoelectron spectroscopy (XPS) equipped with an Al Ka radiation source was used to scan the surface of the prepared catalyst. Catalyst composition was identified by Energy Dispersive Spectroscopy (EDS). The surface morphology and particle sizes of the prepared catalyst were identified using a transmission electron microscope (TEM; JEOL 1230) and a scanning electron microscope (SEM; Hitachi S-4800) with a Bruker EDS detector. The specific surface area of the prepared catalyst was measured using the Brunauer−Emmett−Teller (BET) adsorption isotherm technique. Catalyst powder or pellets were first degassed for three hours at 110 °C. Then, the seven-point BET isotherm method was used to measure the surface area using N_2 gas as the adsorbate using a Quantachrome NOVA 4200e Analyzer. More details about the instruments used in this work are available elsewhere [21]. Diffuse reflectance infrared Fourier transform spectroscopy (DRIFTS) was used to identify the hydroxyl group on the surface of the prepared catalyst, and the spectra were recorded in the range of 2500–4000 cm^{-1}. The procedure of preparing a solid sample and scanning it by DRIFTS is reported elsewhere [22].

2.3. ETB Process

The catalyst activity was evaluated using the catalyst in the ETB process using a fixed bed stainless steel reactor with a continuous upstream flow with an inner diameter and length of 2 and 85 cm, respectively. The reactor is consisted of two parts. The lower part is to evaporate and preheated the feed to the desired temperature, and the upper part is the reaction section. Two heating tapes (Isotherm International) with a two-meter length and a power of 420 W for each were used to heat the reactor to the desired temperature. To control the temperature and keep it constant at the desired level, an indicator and controller (TIC) with a K-type sensor were applied. The gases produced from the reactor were analyzed by an in-situ gas chromatograph (GC) equipped with a CP-PoraPLOT QHT column using an FID detector.

The reaction temperature was chosen in the range 350–450 ◦C under atmospheric pressure based on the literature [3, 19, 23] using 3.95 g of the prepared catalyst. The bottom half of the reactor was covered by a layer of quartz wool and then packed with silica carbide (SiC, 150–400 mesh particle size from Sigma-Aldrich). Then two rings with multi nano-holes, which prevent nanoparticles from passing through them but allow for gases to do so were placed on the top of SiC, and the catalyst powder was inserted between them. The upper half of the reactor was filled with more SiC, which helps to prevent the thermal decomposition of ethanol to acetaldehyde [19]. Each experiment was duplicated, and good reproducibility was observed. The average values were considered.

Generally, some byproducts were formed, such as acetaldehyde, ethylene, trace amounts of carbon oxides, C_1–C_8 hydrocarbons, and other C_3–C_4 oxygenated compounds. Therefore, carbon balance was performed based on the total carbon amount detected in the analysis, divided by the total carbon used, and a good matching was observed. Catalyst coking was not observed. Ethanol conversion was calculated as the mole percent of reacted ethanol to the total ethanol moles fed to the process. In contrast, the product yield was calculated as the mole percent of the ethanol converted to the product that was fed to the process.

3. RESULTS AND DISCUSSION

3.1. Catalyst Nanoparticle Characterization

The BET surface area analysis showed that the synthesized catalyst has a surface area of 442 (m^2 g^{-1}). This high surface area is probably provided by SiO_2, [24] which is confirmed by SEM images which showed a lot of tiny SiO_2 particles that covered each MgO particle, as seen in Figure 1-a. The BET surface area of MgO-SiO_2 pellets is 224 ($m^2.g^{-1}$). EDS analysis for the catalyst showed that Mg, Si, and O concentrations in the prepared catalyst were 22 wt %, 24 wt%, and 54 wt%, respectively, which means that the total percentage of MgO is 50%. Figure 1 (b-d) shows the EDS analysis map of MgO-SiO_2 catalyst where (b) is the distribution of magnesium element, (c) silica element, and (d) oxygen element. This map confirms the homogeneity of the prepared catalyst.

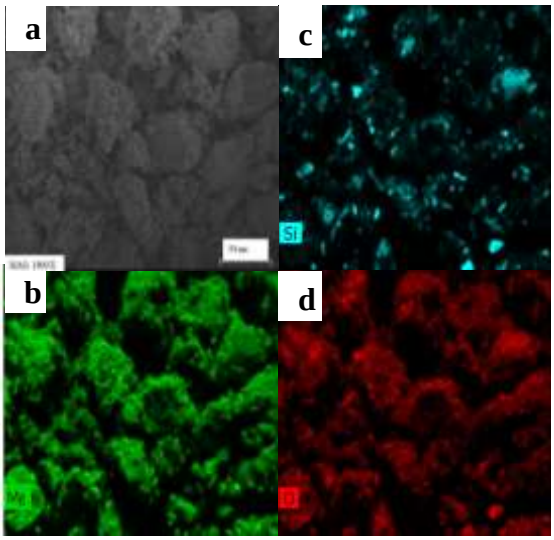

Figure 1. *(a) The SEM image of the synthesized MgO-SiO_2 sample used to generate the EDS images. EDS analysis map of MgO-SiO_2 showing the distribution of (b) magnesium element, (c) silica element, and (d) oxygen elements.*

To identify the surface chemical composition, the catalyst sample was scanned by XPS analysis (Fig. 2). The scan of the Mg 1s region shows only one peak at the binding energies of 1305 eV, which indicates the existence of only one phase of Mg in the form of Mg^{2+} (Fig. 2a) [25]. The oxygen region analysis shows a wide peak that can be fitted into two peaks, as shown in Figure 2-b. The high-intensity peaks centered at 531.1 eV are attributed to the lattice oxygen, while the other peak observed at 532.1 is assigned to the surface hydroxyl group. A peak observed at 103.5 eV in the Si 2p region (Fig. 2c) is assigned to Si^{4+} [26]. From XPS analysis, it can conclude that MgO and SiO_2 are presented in the composites with surface hydroxyl groups. To confirm this conclusion, DRIFTS analysis was used to scan the catalyst powder in the hydroxyl region. As shown in Figure 3-a, a wide peak centered at a wavelength 3400 cm^{-1} resulting probably from adsorption of environmental moisture is observed with two small peaks at wavelengths 3717 and 3628 cm^{-1}, which are assigned to surface hydroxyl groups [27]. To confirm this assignment, the sample was heated to 400 ^oC and scanned by in-situ DRIFTS, where the wide peak assigned to adsorbed water was minimized, and that allowed the other two peaks assigned to the hydroxyl groups to appear clearly. Powder XRD scan of the prepared catalyst (Fig. 3-b) shows a broad diffraction peak at 22^o (2Θ) attributed to amorphous silica with three sharp peaks assigned to MgO, which indicates a good crystalline for MgO particles [28]. The medium calcination temperature used in this work helped to avoid the formation of $MgSiO_4$, which could reduce the surface area and lowers the catalyst activity, as demonstrated by Zhu et al. [29]. In their work, Zhu et al. found that increasing the calcination temperature of the catalyst increases its reactivity with an obvious increasing in the acid-base sites. However, they found that a higher calcination temperature than 500 ^oC resulted in minimized the selectivity towards BD with the obvious formation of $MgSiO_4$ at 700 ^oC. From TEM images analysis (Fig. 3-c as an example), the average projected area

diameter of the catalyst particles before the reaction was 45 (± 10) nm.

3.1. ETB Process

The catalyst activity was evaluated by applying it in the ETB process and investigating the impact of several operating parameters on the catalyst's reactivity for ethanol conversion and product selectivity. Fig. 4-a shows the effect of the temperature on ethanol conversion and product yields.

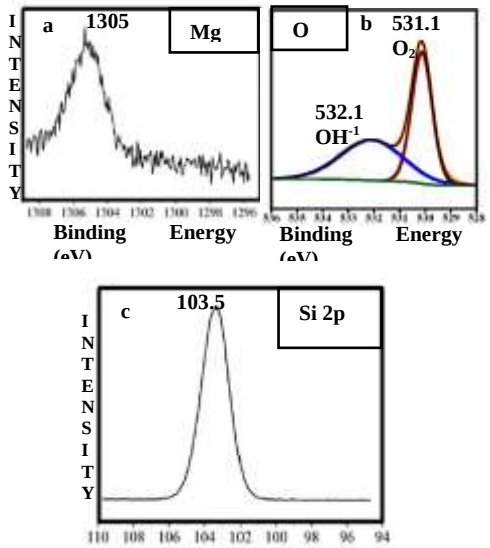

Figure 2. *XPS analysis of prepared MgO-SiO_2 shows (a) Mg 1S, (b) O 1s, and (c) Si 2p regions.*

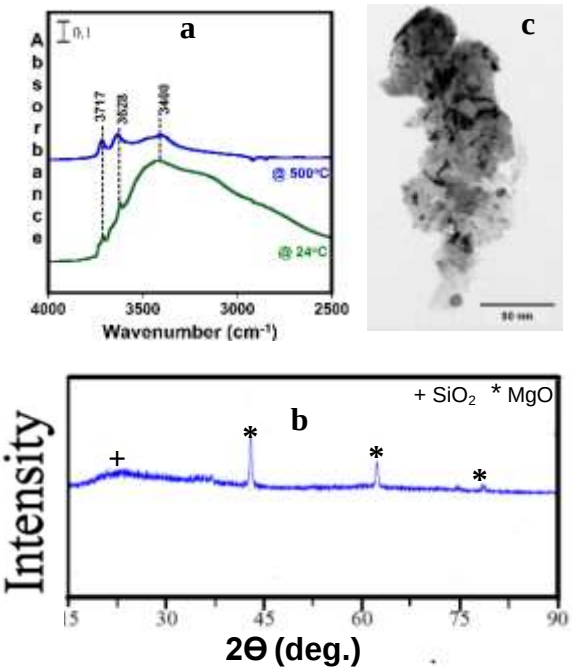

Figure 3. *Characterization of prepared MgO-SiO_2 catalyst(a) DRIFTS scan in the range 2500-4000 cm^{-1}, (b) XRD, and (c) TEM.*

Acetaldehyde, BD, and ethylene were the main products, and the other compounds such as carbon oxides, ethyl acetate, and acetic acid were barely detected due to their low concentrations. As shown in Fig. 4-a, ethanol conversion over MgO-SiO_2 catalyst was enhanced by increasing the reaction temperature. The selectivity of the desired product (BD) did not exceed 10% at the lowest temperature, but it increased with increasing temperature to reach its maxim in value (60%) at 400 ^{o}C. The further increase of temperature above 400 ^{o}C decreased the selectivity of BD and acetaldehyde, while increasing the selectivity towards ethylene and carbon oxides due to the differences in the thermodynamic of these processes as reported in the literature [30, 31]. The continuous increase in the ethylene selectivity with persistence decreasing in acetaldehyde selectivity with increasing reaction temperature indicates that ethylene and acetaldehyde follow different parallel competitive reaction pathways. The difference in the reaction pathway is due to the different types of active sites, which are needed for these reactions. Specifically, acidic sites are required for the formation of ethylene, and basal sites are required for the formation of acetaldehyde. The optimum reaction temperature of 400 ^{o}C was considered in the following experiments investigating the effect of the weight hourly space velocity and water content.

Figure 4-b shows the effect of increasing the flow rate of ethanol feeding to the reactor from 0.01 to 0.04 (l. h^{-1}), which resulted in increasing the weight hourly space velocity (WHSV) from 2 to 4 (h^{-1}). Increasing the feed flow rate resulted in decreased ethanol conversion and the selectivity of BD, ethylene, and carbon oxides. On the other hand, acetaldehyde

selectivity increased with increasing the feed flow rate. The reduction in ethanol conversion with elevating the WHSV is attributed to decreasing the contact time [32]. The reduction in the selectivity of BD and ethylene versus the increase in the acetaldehyde selectivity with increasing the feed flow rate confirms two conclusions. First, the acetaldehyde forms as an intermediate in the formation of BD, and reducing the contact time limits the further conversion of acetaldehyde to BD [33]. Second, it confirms the previous conclusion that ethylene forms in a different path than acetaldehyde.

Figure 4-c shows the impact of diluting the ethanol with water at the optimum temperature and flow rate. Water presence increases the ethanol conversion but lowers the selectivity towards BD and ethylene. At the same time, acetaldehyde selectively increased with increasing water content. In addition, acetone formation was observed with increasing the water content. The first step in the ETB reaction mechanism is the ethanol dehydrogenation to acetaldehyde. The suggested reaction mechanism (Fig. 5) [34] assumes that acetaldehyde forms crotonaldehyde by aldol condensation, which in turn hydrogenated by the hydrogen produced during the dehydrogenation step of ethanol, resulting in the formation of crotyl alcohol which considers an intermediate of BD [23]. The last step is the dehydration reaction which leads to forming BD. Thus, the presence of water in the feedstock limits the dehydration step, which results in preventing the conversion of acetaldehyde to BD. Acetone formation is due to the modification of the active sites of aldol condensation by H_2O, resulting in the process of keto-enol tautomerization of acetaldehyde [35, 36]. This result is agreed well with that of Ochoa et al., who noticed a poising effect for the water on the catalyst, resulting in decreasing the BD selectivity [1]. However, Zhu et al., found that diluting ethanol with water in a low percentage can increase the selectivity to BD. In contrast, they found that the higher water percentages, such as those used in this investigation, reduce the BD selectivity [29].

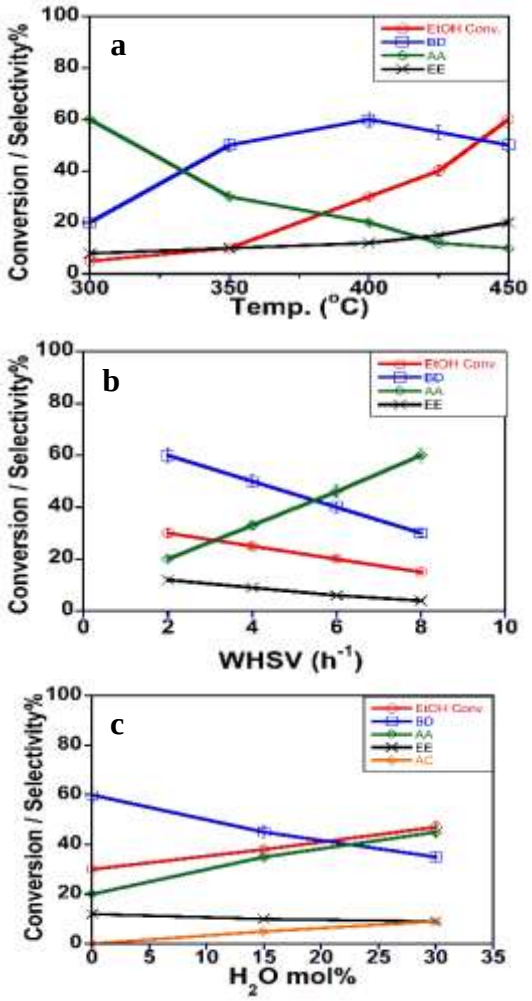

Figure 4. *Investigation of the impact of (a) Temperature, (b) WHSV (h-1), and (c) water content on the performance of the prepared catalyst in ETB process.*

The superior activity of the prepared catalyst in this work compared with literature is attributed to the morphology of MgO-support interaction, as determined by catalyst characterization. Specifically, the heterogeneous ETB reaction that occurs either on the Lewis or basal sites, resulting from the interaction of MgO as a source of basal sites with SiO_2, which provides Lewis sites. The presence of two hydroxyl groups on the surface of the prepared catalyst indicates the enrichment of the catalyst surface with basal sites, which are

very appreciative in this reaction. This confirmed the importance of the catalyst surface chemistry in its activity for BD production. This finding agrees with the literature [29, 37].

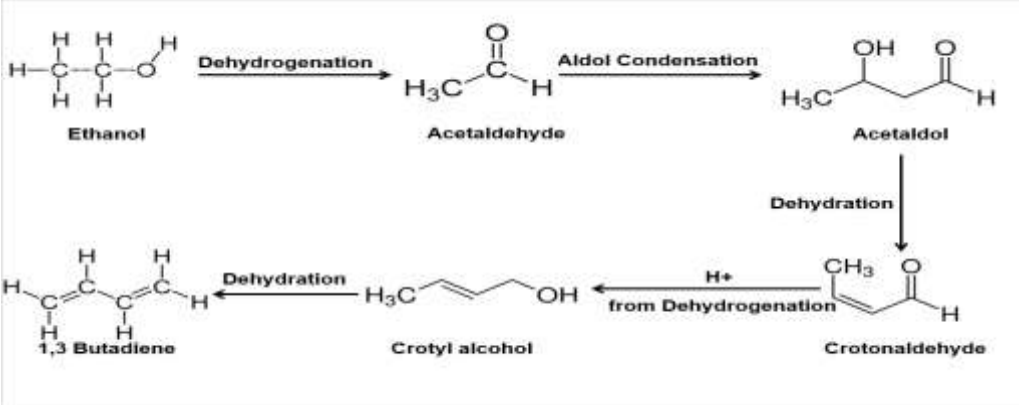

Figure 5. *Proposed reaction mechanism of ethanol conversion to 1,3 butadiene*

In addition, the high surface area provided by the nanoparticle size plays an essential role in the high reactivity of the prepared catalyst. Reschetilowski et al. reported achieving around 50% BD selectivity using particle sizes between 200-400 µm [38]. Taifan and Baltrusaitis reported 29.7% BD selectivity using pellet sizes between 100-150 µm [39]. These values are lower than that achieved in the current work using nanoparticles. To confirm the importance of the catalyst particle size on the reactivity, the synthesized powder was compressed to pellets of the size 500 µm and then applied in the reaction at the optimal reaction conditions. Figure 6 compares the performance of the nanoparticles and pellets in term of ethanol conversion and BD selectivity for ten hours. As seen in Figure 6, the performance of nanoparticles is superior for BD production and ethanol conversion. The higher reactivity of nanoparticles than that of pellets is probably due to the higher surface area provided by nanoparticles. From Figure 6, it can be seen both sample sizes have good stability with time, where only 4-10% of the selectivity was lost during the reaction period. The loss in the catalyst reactivity is probably due to the poising effect of resulted water [1].

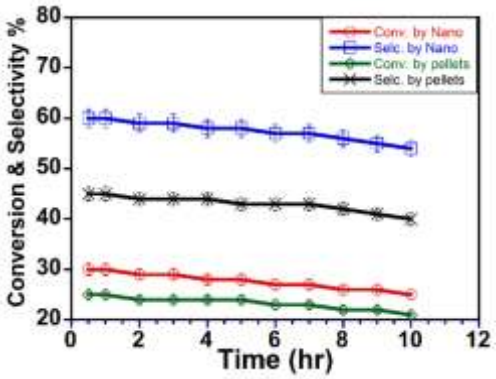

Figure 6. *Comparison of reactivity and stability of MgO-SiO_2 nanoparticles and pellets at 400 ^oC, WHSV=2 (h^{-1}), catalyst weight = 3.95 g, and no water presence.*

4. CONCLUSIONS

Characterization of prepared MgO-SiO_2 by TEM and BET shows that dropping the particle sizes to the nanoscale provides a high surface area, which is a critical criterion for any catalyst. XRD scan confirms the good crystallinity of the MgO phase while SiO_2 is in the amorphous phase because of the medium calcination temperature used, which helped to prevent the formation of $MgSiO_4$ that could reduce the surface area and lowers the catalyst activity. The XPS and DRIFTS investigations confirm the presence of two hydroxyl groups on the surface which enhances the basicity of the catalyst and increases its activity in the ETB process, which requires both basal and Lewis sites.

In general, increasing the reaction temperature increases the selectivity of BD and ethylene, and ethanol conversion, while decreasing the selectivity of acetaldehyde which indicates that ethylene and acetaldehyde are formed as byproducts in different pathways. However, the further increase of the temperature beyond 400 ^{o}C reduces the selectivity of BD and acetaldehyde and increases the selectivity of ethylene. Increasing the feed flow rate decreases the selectivity of both BD and ethylene while increasing the selectivity of acetaldehyde. This confirms that acetaldehyde is formed as an intermediate component for BD and in different pathways from ethylene, which is formed as a byproduct. The presence of water in the feedstock increases the acetone formation rate, resulting in an increasing in the total conversion of ethanol, but with lower selectivity towards the formation of BD.

ACKNOWLEDGEMENT

The authors wish to thank Al-Mustaqbal College University for its financial supporting of authors

CONFLICT OF INTEREST

The authors declare that they have no conflict of interest.

REFERENCES

1. Ochoa, J. V., Bandinelli, C., Vozniuk, O., Chieregato, A., Malmusi, A., Recchi, C., Cavani, F., "An analysis of the chemical, physical and reactivity features of MgO–SiO_2 catalysts for butadiene synthesis with the Lebedev process", *Green Chemistry,* 18 (2016) 1653-1663.
2. Mohammed, M. M., Ali, N. S. M., Alalwan, H. A., Alminshid, A. H., Aljaafari, H. A., "Synthesis of ZnO-CoO/Al_2O_3 nanoparticles and its application as a catalyst in ethanol conversion to acetone", *Results in Chemistry*, 3 (2021) 100249.
3. Makshina, E., Janssens, W., Sels, B., Jacobs, P., "Catalytic study of the conversion of ethanol into 1, 3-butadiene", *Catalysis Today*, 198 (2012) 338-344.
4. Liguras, D. K., Kondarides, D., Verykios, X., "Production of hydrogen for fuel cells by steam reforming of ethanol over supported noble metal catalysts", *Applied Catalysis B: Environmental,* 43 (2003) 345-354.
5. Frusteri, F., Freni, S., Spadaro, L., Chiodo, V., Bonura, G., Donato, S., Cavallaro, S., "H_2 production for MC fuel cell by steam reforming of ethanol over MgO supported Pd, Rh, Ni and Co catalysts", *Catalysis Communications,* 5 (2004) 611-615.
6. Posada, J., Patel, A., Roes, A., Blok, K., Faaij, A., Patel, M., "Potential of bioethanol as a chemical building block for biorefineries preliminary sustainability assessment of 12 bioethanol-based products", *Bioresource technology,* 135 (2013) 490-499.
7. Cespi, D., Passarini, F., Vassura, I., Cavani, F., "Butadiene from biomass, a life cycle perspective to address sustainability in the chemical industry", *Green Chemistry,* 18 (2016) 1625-1638.
8. Moncada, J., Gursel, I., Worrell, E., Ramírez, A., "Production of 1, 3-butadiene and ε-caprolactam from C6 sugars: Techno-economic analysis" *Biofuels, Bioproducts and Biorefining,* 12 (2018) 600-623.
9. Kyriienko, P., Larina O., Soloviev, S., Orlyk, S., Calers, C., Dzwigaj, S., "Ethanol conversion into 1, 3-butadiene by the Lebedev method over MTaSiBEA zeolites (M= Ag, Cu, Zn)", *ACS Sustainable Chemistry & Engineering,* 5 (2017) 2075-2083.
10. Alalwan, H. A., Alminshid, A. H., "CO_2 Capturing Methods: Chemical Looping Combustion (CLC) as a Promising Technique", *Science of The Total Environment,* 788 (2021) 147850.
11. Ezinkwo, G., Tretyakov, V., Aliyu, A., Ilolov, A., "Fundamental Issues of Catalytic Conversion of Bio-Ethanol into Butadiene", *ChemBioEng Reviews,*1 (2014) 194-203.
12. Jones, M., Keir, C., Di Iulio, C., Robertson, R., Williams, C., Apperley, D., "Investigations into the conversion of ethanol into 1, 3-butadiene", *Catalysis Science & Technology,* 1 (2011) 267-272.
13. Da Ros, S., Jones, M., Mattia, D., Pinto, J., Schwaab, M., Noronha, F., Kondrat, S., Clarke, T., Taylor, S. "Ethanol to 1, 3-butadiene conversion by using ZrZn-containing MgO/SiO_2 systems prepared by co-precipitation and effect of catalyst acidity modification", *ChemCatChem,* 8 (2016) 2376-2386.
14. Makshina, E., Dusselier, M., Janssens, W., Degreve, J., Jacobs, P., Sels, B. "Review of old chemistry and new catalytic advances in the on-purpose synthesis of butadiene", *Chemical Society Reviews,* 43 (2014) 7917-7953.
15. Subhan, M., Chandra Saha, P., Uddin, N., Sarker, P. "Synthesis, structure, spectroscopy and photocatalytic studies of nano multi-metal oxide MgO· Al_2O_3· ZnO and MgO· Al_2O_3· ZnO-curcumin composite", *International Journal of Nanoscience and Nanotechnology,* 13 (2017) 69-82.

16. Amirmoghadam, H., Aghabozorg, H., Hossaini Sadr, M., Salehirad, F., Irandoukht, A. "The Effect of Different Supports on the Characteristic and Catalytic Properties of Ni-Mo/Cs1. 5H1. 5PW12O40/S (S= SiO_2 or Al_2O_3 or ASA) Nanocatalysts in Hydrocracking of n- decane", *International Journal of Nanoscience and Nanotechnology*, 1 (2020) 137-144.
17. Kyriienko, P., Larina, O., Soloviev, S., Orlyk, S., "Catalytic conversion of ethanol into 1, 3-butadiene: achievements and prospects: a Review", *Theoretical and Experimental Chemistry*, 56 (2020) 213-242.
18. Szabó, B., Novodárszki, G., May, Z., Valyon, J., Hancsók, J., Barthos, R., "Conversion of ethanol to butadiene over mesoporous In_2O_3-promoted MgO-SiO_2 catalysts", *Molecular Catalysis*, 491 (2020) 110984.
19. Janssens, W., Makshina, E., Vanelderen, P., De Clippel, F., Houthoofd, K., Kerkhofs, S., Martens, J., Jacobs, P., Sels, B., "Ternary Ag/MgO-SiO_2 Catalysts for the Conversion of Ethanol into Butadiene", *ChemSusChem*, 8 (2015) 994-1008.
20. Alalwan, H. A., Alminshid, A. H., Mohammed, M. M., Mohammed, M. F., "Reviewing of using Nanomaterials for Wastewater Treatment", *Pollution*, 8 (2022) 995-1013.
21. Alalwan, H. A., Augustine, L. J., Hudson, B. G., Abeysinghe, J. P., Gillan, E. G., Mason, S. E., Grassian, V. H., Cwiertny, D. M., "Linking Solid-State Reduction Mechanisms to Size-Dependent Reactivity of Metal Oxide Oxygen Carriers for Chemical Looping Combustion", *ACS Applied Energy Materials*, 4 (2021) 1163-1172.
22. Alalwan, H. A., Alminshid, A. H., "An in-situ DRIFTS study of acetone adsorption mechanism on TiO_2 nanoparticles", *Spectrochimica Acta Part A: Molecular and Biomolecular Spectroscopy*, 229 (2020) 117990.
23. Szabó, B., Novodárszki, G., Pászti, Z., Domján, A., Valyon, J., Hancsók, J., Barthos, R., "MgO-SiO_2 Catalysts for the Ethanol to Butadiene Reaction: The Effect of Lewis Acid Promoters", *ChemCatChem*, 12 (2020) 5686-5696.
24. Ma, R., Cui, B., Hu, D., Wang, Y., Zhao, W., Tian, M., "Improving the Dielectric Properties of the Ba (Zr0. 1Ti0. 9) O3-based Ceramics by Adding a Li2O–SiO2 Sintering Agent Step by Step," *International Journal of Nanoscience and Nanotechnology*, 16 (2020) 233-241.
25. García, L., Mendivil, M., Roy, T., Castillo, G., Shaji, S., "Laser sintering of magnesia with nanoparticles of iron oxide and aluminum oxide", *Applied Surface Science*, 336 (2015) 59-66.
26. Tan, R., Azuma, Y., Kojima, I., "Comparative study of the interfacial characteristics of sputter-deposited HfO_2 on native SiO_2/Si (100) using in situ XPS, AES and GIXR", *Surface and Interface Analysis: An International Journal devoted to the development and application of techniques for the analysis of surfaces, interfaces and thin films*, 38 (2006) 784-788.
27. Alminshid, A. H., Abbas, M. N., Alalwan, H. A., Sultan, A. J., Kadhom, M. A., "Aldol condensation reaction of acetone on MgO nanoparticles surface: An in-situ drift investigation", *Molecular Catalysis*, 501 (2021) 111333.
28. Xu, Z., Yu, J., Liu, G., Cheng, B., Zhou, P., Li, X., "Microemulsion-assisted synthesis of hierarchical porous Ni $(OH)_2$/SiO_2 composites toward efficient removal of formaldehyde in air", *Dalton Transactions*, 42 (2013) 10190-10197.
29. Zhu, Q., Wang, B., Tan, T., "Conversion of ethanol and acetaldehyde to butadiene over MgO–SiO_2 catalysts: effect of reaction parameters and interaction between MgO and SiO_2 on catalytic performance", *ACS Sustainable Chemistry & Engineering*, 5 (2017) 722-733.
30. Gucbilmez, Y., Dogu, T., Balci, S., "Ethylene and acetaldehyde production by selective oxidation of ethanol using mesoporous V− MCM-41 catalysts", *Industrial & engineering chemistry research*, 45 (2006) 3496-3502.
31. Abdulrazzaq, H., Rahmani Chokanlu, A., Frederick, B., Schwartz, T., "Reaction Kinetics Analysis of Ethanol Dehydrogenation Catalyzed by MgO–SiO_2", *ACS Catalysis*, 10 (2020) 6318-6331.
32. Alalwan, H. A., Mohammed, M. M., Sultan, A. J., Abbas, M. N., Ibrahim, T. A., Aljaafari, H. A., Alminshid, A. H., "Adsorption of methyl green stain from aqueous solutions using non-conventional adsorbent media: Isothermal kinetic and thermodynamic studies", *Bioresource Technology Reports*, 14 (2021) 100680.
33. González, G., Concepción, P., Perales, A., Martínez, A., Campoy, M., Vidal-Barrero, F., "Ethanol conversion into 1, 3-butadiene over a mixed Hf-Zn catalyst: Effect of reaction conditions and water content in ethanol", *Fuel Processing Technology*, 193 (2019) 263-272.
34. Zhao, Y., Li, S., Wang, Z., Wang, S., Wang, S., Ma, X., "New ZnCe catalyst encapsulated in SBA-15 in the production of 1, 3-butadiene from ethanol", *Chinese Chemical Letters*, 31 (2020) 535-538.
35. Cantú, F. G., Barman, P., Mukherjee, G., Kumar, J., Kumar, D., Kumar, D., Sastri, C., de Visser, S., "Keto–enol tautomerization triggers an electrophilic aldehyde deformylation reaction by a nonheme manganese (III)-peroxo complex", *Journal of the American Chemical Society*, 139 (2017) 18328-18338.

36. Couch, D., Nguyen, Q., Liu, A., Hickstein, D., Kapteyn, H., Murnane, M., Labbe, N., "Detection of the keto-enol tautomerization in acetaldehyde, acetone, cyclohexanone, and methyl vinyl ketone with a novel VUV light source", *Proceedings of the Combustion Institute*, 38 (2021) 1737-1744.
37. Huang, X., Men, Y., Wang, J., An, W., Wang, Y., "Highly active and selective binary MgO–SiO_2 catalysts for the production of 1, 3-butadiene from ethanol", *Catalysis Science & Technology*, 7 (2017) 168-180.
38. Reschetilowski, W., Hauser, M., Alscher, F., Klauck, M., Kalies, G., "Studies on the Binary MgO/SiO_2 Mixed Oxide Catalysts for the Conversion of Ethanol to 1, 3-Butadiene", *Catalysts*, 10 (2020) 854.
39. Taifan, W., Baltrusaitis, J., "In Situ Spectroscopic Insights on the Molecular Structure of the MgO/SiO_2 Catalytic Active Sites during Ethanol Conversion to 1, 3-Butadiene", *The Journal of Physical Chemistry C*, 122 (2018) 20894-20906.